Vision Res. Vol. 26, No. 4, pp. 643–652, 1986
Printed in Great Britain.

0042-6989/86 $3.00 + 0.00

SMOOTH AND SAMPLED MOTION

DAVID C. BURR, JOHN ROSS and M. CONCETTA MORRONE
Department of Psychology, University of Western Australia, Perth, WA 6009, Australia

(*Received* 6 *May* 1985; *in revised form* 3 *October* 1985)

Abstract—Stroboscopic or sampled motion is indistinguishable from smooth motion if the frequency of sampling is sufficiently high. We report measurements of the minimum sample frequency for smooth motion of drifting sinusoidal gratings (extended and truncated) which varied in spatial frequency from 0.06 to 24 c/deg, in temporal frequency from 1.5 to 24 Hz and in contrast from 3 to 100 times detection threshold. Threshold sampling frequency for smoothness increased with temporal frequency and contrast, and inversely with spatial frequency. The threshold step size associated with the sampling frequency ranged from 20″ arc (for gratings of 24 c/deg) to 6 deg (for gratings of 0.06 c/deg). Calculations of the spurious frequencies introduced by sampling lead us to conclude that motion appears smooth provided that sampling is above the Nyquist limit and that the amplitude of the spurious components is below their independent threshold.

Vision Stroboscopic motion Sampling Sinusoidal gratings Apparent motion

INTRODUCTION

The only means we have to record motion so that it can be viewed remotely in space or time are to sample it and display the samples as still pictures in sequence. The motion that we then see has been termed apparent motion and our ability to see motion when viewing cinema or television has often been regarded as mysterious and dependent on means other than those by which we see real motion. Indeed the Gestalt movement, and Wertheimer (1912) in particular, took it to be self-evident that the appearance of movement was something added to a sequence of stills by the observer. This apparently paradigm case of the Gestalt going beyond the sum of its constituent parts was made a central plank of the Gestalt platform.

It has widely been assumed that the motion seen in cinematic motion sequences is derived from an analysis of the samples as stills by some kind of computation (Ullman, 1979; Marr and Ullman, 1981) or even cognitive (Johannson, 1975) process. Attempts have been made to distinguish apparent from real motion by various criteria (Kolers, 1972) and more recently a distinction has been drawn between two processes supposed to underlie apparent motion, one a short range process operating up to 15 min (Braddick, 1974), or a little more (Baker and Braddick, 1982; Chang and Julesz, 1983; Nakayama and Silverman, 1984); the other a long range process operating up to 1 or 2 deg, or even several degrees (Zeeman and Roelofs, 1953).

Cinematic, stroboscopic, and other sequences giving rise to the appearance of motion may be viewed as ways of sampling and thus preserving information about motion while introducing artefacts due to sampling (Pearson, 1975). The region within which human vision responds with contrast sensitivity 100 or more can be represented as an oval on the spatio-temporal Fourier plane, having a central void. The void represents the cut in sensitivity at frequencies low both spatially and temporally. Burr (1979) used this representation of visual sensitivity to explain why continuous motion appears smeared at short exposures (sampling spreads the spectrum, alerting stasis channels), and why stroboscopic sequences may mimic smooth motion, especially when high spatial frequencies are attenuated by blurring.

Fahle and Poggio (1981) analysed two types of stroboscopic sequence in more detail in terms of components of sampled motion and support on the Fourier plane for motion sensitive channels: "We imagine, following Burr (1979), that these channels have somewhat overlapping supports covering the region of the f_x–f_t Fourier plane which corresponds to the sensitive range of the visual system" (p. 466). They went on to show how motion channels may interpolate sampled to smooth motion by filtering out the side lobes arising from coarse spatial sampling. In terms similar to those used by Burr (1979) and by Fahle and Poggio (1981), Watson, Ahumada and Farrell (1983) portrayed the "window of visibility" (Campbell, 1980, p. 326) on the Fourier plane in simplified separable form as a rectangle with no void. Like Fahle and Poggio (1979) they analysed stroboscopic motion into its spectral components, explicitly concluding that sampled and smooth motion are indistinguishable when the components distinguishing them escape detection.

Here we approach the problem of apparent motion as a matter of sampling, having in mind the question: when is sampled motion indistinguishable from continuous (or smooth) motion? We examine drifting gratings and moving wave packets of a wide range of different sizes, speeds and contrasts to establish the sampling limits at which smooth and sampled motion match one another in appearance.

METHODS

Two types of stimuli were used in these experiments: vertical sinusoidal gratings and Gabor packets (sinusoidal gratings multiplied by a Guassian, illustrated in the inset of Fig. 4). Both types were generated by computer (Cromenco Z80) and displayed on a cathode ray oscilloscope having its own internal raster (Joyce Electronics, Cambridge), set at 200 frames/sec, 600 lines/frame. The space-average luminance remained at 400 cd/m^2 throughout the series of experiments. Gratings and wave packets were caused to drift by periodically repositioning them on the screen. After each repositioning, they were held in that position for a fixed time before further repositioning. We refer to this process as "sample and hold". By this means it was possible to adjust the frequency of sampling (the inverse of the duration between repositioning) of a grating or wave packet moving at any desired velocity. Granularity of adjustment (and approximation to continuous motion) was set by the frame-plus-flyback period of 5 msec.

All grating measurements were made with 4 cycles of grating on the screen (30 × 22 cm), giving them a constant spatial frequency of 0.13 c/cm. Spatial frequency at the eye was varied by changing viewing distance over a range from 25 cm to 103 m and temporal frequency set at 1.5, 3, 6 or 12 Hz directly by the computer. The screen was covered with tight fitting onion paper so as to render invisible the raster lines of the display at the closest viewing distances. Intermediate viewing distances were achieved by observing the screen's reflection in a front silvered mirror, and the two longest by looking through binoculars (Zeiss 10 × 25B) in reverse. All observations were made with two eyes.

In the main series of experiments measurements were made at four contrast levels: at 3, 10, 30 and 100 times the observer's contrast threshold for detecting the particular pattern in motion. The experiment comprised two parts: for each viewing distance the observer first adjusted the contrast of a grating in smooth motion to determine his detection threshold at each of 4 temporal frequencies. These values were used to calculate the actual contrasts employed. The computer then displayed in random order at each viewing distance stimuli at the four temporal frequencies and at each of the four calculated levels of contrast. The next task of the observer was to adjust the frequency at which the moving grating was sampled to determine the minimum frequency at which the appearance of sampled motion matched exactly the appearance of smooth motion. Equivalently the observer could be said to have adjusted the jump size between successive positions of the sampled grating, since the jump size varies inversely with the sampling frequency (and directly with velocity)

$$v = F_t/F_s = S_f \cdot S_j \qquad (1)$$

where v is velocity, F_t the temporal frequency of drift, F_s the spatial frequency of the grating, S_f the sample (temporal) frequency and S_j the jump size.

Adjustments were made with a hand-held rotary switch read by the computer. Five measurements were made at each combination of spatial frequency, temporal frequency and contrast, from which a mean and standard error were calculated. To make matches the observer had a button to switch between sampled and continuous motion and was encouraged to use it frequently.

Procedures for Gabor wave packets were similar except that the packet swept once across the screen and then was held the time taken by the sweep before being swept across again.

Observers allowed each stimulus to sweep by many times, while adjusting sampling frequency (or step size), before concluding a match. Forced choice procedures were not used because limited exposure times, required by such techniques, introduce additional sampling artefacts (Burr, 1979).

In supplementary experiments with gratings, sampling frequency was fixed by the computer and subjects asked to adjust contrast to find the level of contrast (if one existed) at which sampled motion was indistinguishable from smooth.

RESULTS

We report first results of measurements with drifting gratings. Figures 1 and 2 show for the two observers the maximal jump size at which sampled is indistinguishable from smooth motion, for gratings of various spatial and temporal frequency and contrasts. The maximum jump size is affected by all three parameters. There is, at each temporal frequency, a very large effect of spatial frequency (more than two log units) and a smaller effect of contrast. The higher the spatial frequency of the drifting grating, the smaller the maximal jump size at which it appears smooth when sampled. The maximum permissible jump size is smaller at high contrast than at low, and the effect of contrast is slightly greater at low spatial frequencies, declining as spatial frequency increases. Temporal frequency itself has a small effect on maximal jump size: the higher the temporal frequency, the greater the maximal permissible jump size. The greatest upper bound

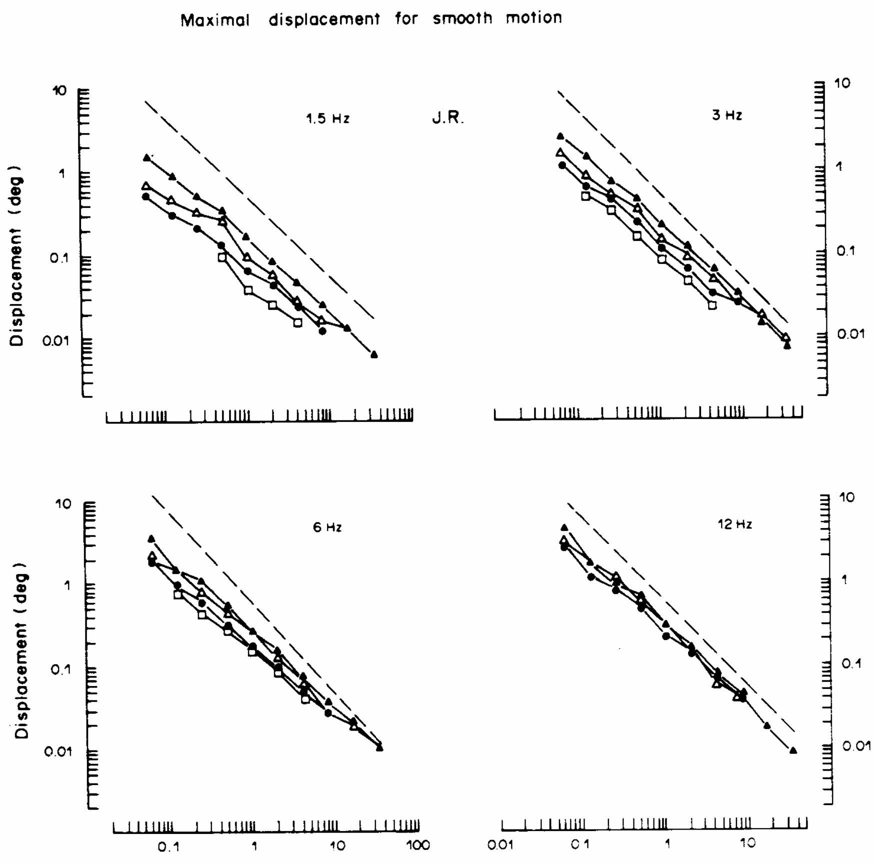

Fig. 1. The maximal displacement between frames (jump size) for seeing smooth motion with sinusoidal gratings of various spatial and temporal frequency and contrasts (▲ 3 times; △ 10 times; ● 30 times; □ 100 times the detection threshold for seeing the grating drift smoothly). The dashed lines show the Nyquist sampling limit, corresponding to half the period of the grating. These results are for observer J.R.

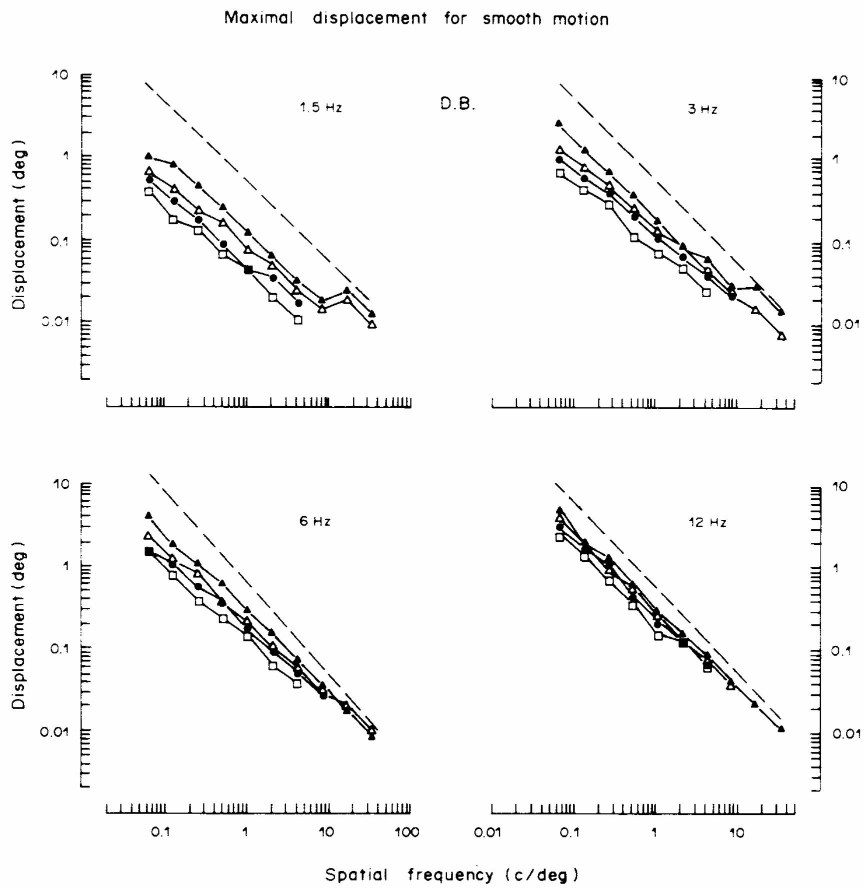

Fig. 2. Same as Fig. 1 for observer D.B.

on jump size for sampled motion to appear smooth is about 6 deg, and the least upper bound is about 0.006 deg. The larger value is found at 3 times threshold contrast for a grating of spatial frequency 0.07 c deg moving at 12 Hz (150 or so deg sec), and the lower at 100 times threshold for a grating of 24 c deg moving at 1.5 Hz (0.06 deg sec).

If a grating jumps more than half its period on each shift, aliasing is introduced and the grating may appear to move backwards like the spokes of a rotating wheel in the cinema or on television. Figures 1 and 2 show the value of this limit (the Nyquist limit) at every spatial frequency as a broken line with a slope of -1. It will be observed that, for each temporal frequency, bounds on jump size fall on curves almost, but not quite parallel to the Nyquist limit line. The curves all converge toward the limit line as spatial frequency increases, and are closer to it at high than at low temporal frequencies.

Figure 3 shows the same grating measurements, for one contrast level (10 times threshold), plotted as temporal frequency of sampling, not jump size [equation (1)]. The Nyquist limit now is expressed as a temporal frequency, double the temporal frequency at which the sampled grating is drifting. Each of the curves in Fig. 3 through the lower bound on sampling frequency (which correspond to the upper bound on jump size) lies above its appropriate Nyquist limit, but drops toward the limit as spatial frequency increases. In no case is the limit reached.

The pattern of results for Gabor wave packets is similar to that for drifting gratings, despite the fact that one is a repetitive pattern giving continuous stimulation and the other is not (cf. Burr and Ross, 1982). Figure 4 shows the upper bound on jump size for wave packets whose fundamental frequency varies over a range from 0.07 to 12 c deg and which drift at (fundamental) temporal frequencies of 1.5, 3, 6, 12 or

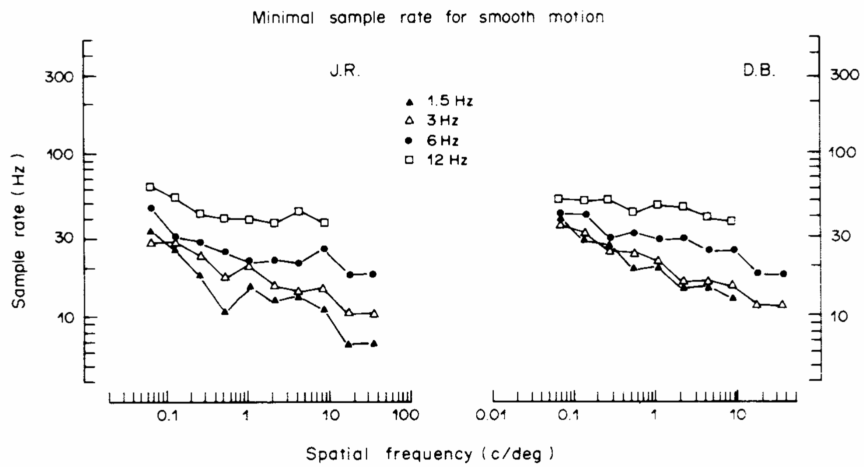

Fig. 3. Some of the results of Figs 1 and 2 (those collected at 10 times detection threshold) replotted as as function of sample rate [see equation (1)]. The drift rates were: 1.5 (▲), 3 (△), 6 (●) and 12 (□) Hz.

32 Hz. At each temporal frequency the upper bound decreases with a slope near −1 over a range of about 2 log units. At each spatial frequency the upper bound, or greatest jump size at which the sweep of the grating looks smooth, increases with temporal frequency. The complete range is from about 3 deg at a fundamental of 0.07 c/deg moving at 24 Hz to just below 0.01 deg (36″) at a fundamental of 16 c/deg moving at 1.5 Hz. The range of permissible jump sizes is less for Gabor wave packets than for gratings. It is slightly truncated both at the bottom and the top ends. Each wave packet contains a range of spatial and hence temporal frequencies having a Gaussian distribution about the fundamental. Truncation at the top end of the scale is presumably due to the higher harmonics which reduce the upper bound on

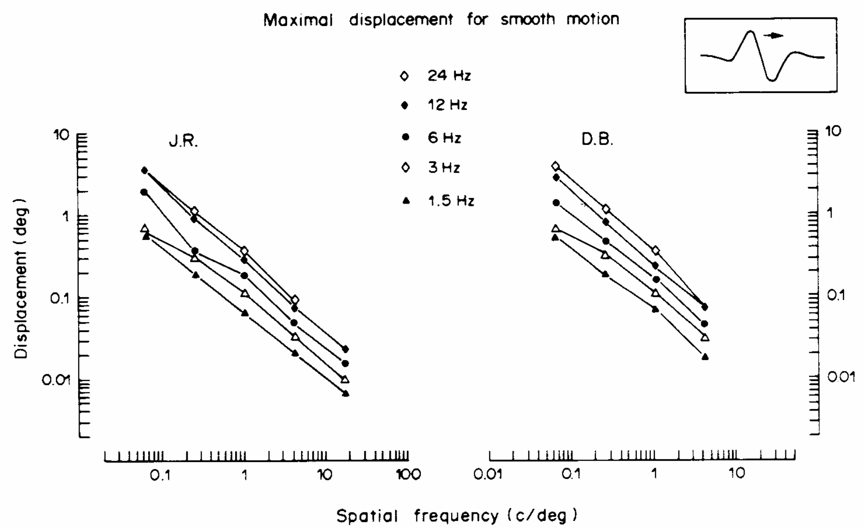

Fig. 4. Threshold displacement to see drifting "Gabor packets" in smooth motion. The inset shows the luminance profile of the waveform used (which was constructed by multiplying a sinusoidal waveform by a Gaussian of sigma equal to half the sinewave period). The fundamental drift frequencies were: 1.5 (▲), 3 (△), 6 (●), 12 (◆), 24 (◇) Hz.

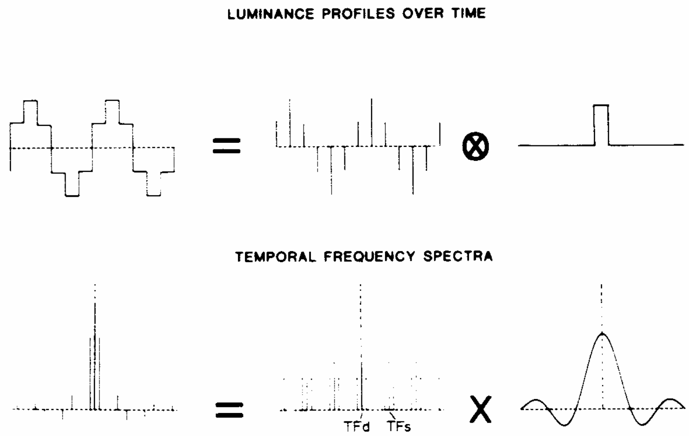

Fig. 5. *Upper row.* Left: luminance variation over time at a single point of the sinusoidal grating of drift frequency TFd after the "sample and hold" procedure. Mathematically the waveform is equal to the convolution of a sinusoidal function periodically sampled at a temporal frequency of TFs (centre), and a pulse function of width 1/TFs (right). *Lower row.* The Fourier Transforms of the above waveforms. The spectrum of the sample and hold waveform (left) is given by the product of the spectra of the sample (centre) and pulse (right) functions. Note that the pulse function spectrum reduces to zero at multiples of TFs, thereby annulling the spurious components related to the sampling of the dc level.

jump size. The explanation for truncation at the lower end of the spatial frequency scale is less obvious.

The last set of results to be reported compares calculated with observed thresholds in order to provide an interpretation of the results presented so far. Figure 5 depicts the luminance changes over time at a fixed point on the screen during sample and hold motion. The luminance is held for a certain time, the sampling period, until it jumps to a new level as the drifting grating is resampled. The luminance profile can be regarded (see Fig. 5) as a convolution in time between a sinusoidal waveform sampled at a frequency of S_f and a pulse function of width $1/S_f$. In the temporal frequency domain the convolution process corresponds to a multiplication of the Fourier transform of the sampled waveform by the transform of the pulse function. The first is a repetitive pattern of spikes repeating about integral multiples of the sample frequency; the second is a sinc function of the form

$$F(\omega) = [\sin(\omega/S_f)]/\omega. \qquad (2)$$

That is to say, the sample and hold process preserves nearly unchanged the mean luminance and the frequency component corresponding to the original grating, and introduces an infinite number of spurious frequencies with decreasing amplitude. The temporal frequency of the first and greatest spurious component is S_f–F_t, and its amplitude (a) is given by

$$a = 1/2\,A \cdot \{\sin[S_f - F_t)/S_f]\}/(S_f - F_t) \qquad (3)$$

where A and F_t are the amplitude and temporal frequency of the drifting grating. Knowing the contrast at which a sampled grating just appears to drift smoothly we can calculate the amplitude and temporal frequency of the major spurious component of motion introduced into the spectrum by sampling.

To test whether the appearance of smooth motion was determined by the spurious frequencies, we measured contrast thresholds for seeing smooth motion. Two sets of measurements were made with gratings of 0.25 and of 8 c/deg. In the first set temporal frequency of drift was fixed at 1.5, 3 or 6 Hz and sampling frequency, for each combination of spatial and temporal frequency, varied by the computer from 10 to 40 Hz. The task of the subject was to adjust the contrast to the highest level at which sampled motion appeared smooth. If smooth motion occurred at no contrast or at all contrasts, the observer signalled this with appropriate buttons. The results are shown in Fig. 6. They reveal that the adjustment was possible only at a limited number of the combinations of size, speed and frequency of sampling used in the experiment.

In the second set of measurements gratings

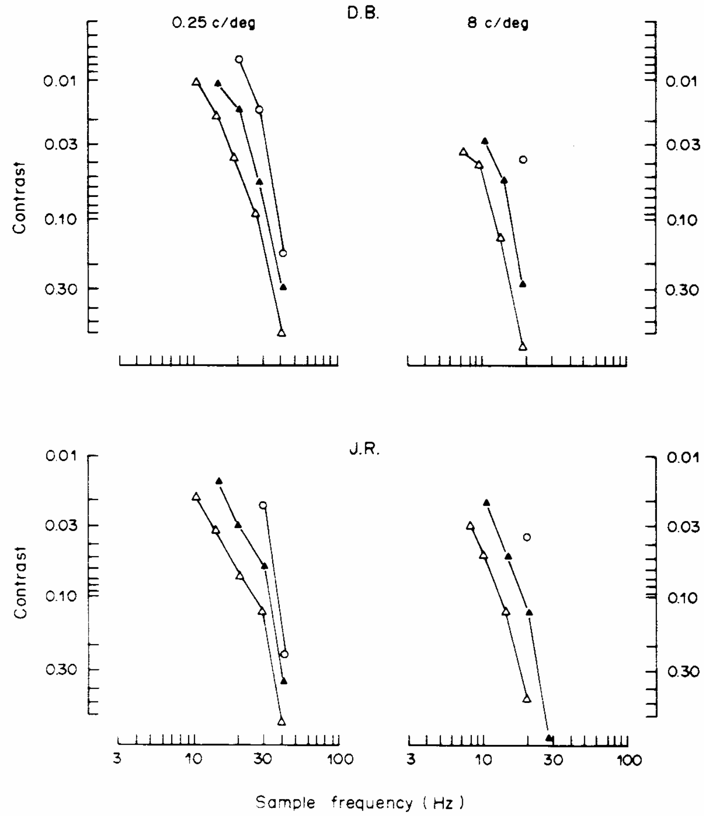

Fig. 6. Threshold contrast for seeing smooth motion in gratings of 0.25 (left) and 8 (right) c deg, as a function of sample rate. The drift rates were 1.5 (△), 3 (▲) and 6 (○) Hz.

of 0.25 and of 8 c/deg were caused to drift smoothly at temporal frequencies closely spaced within a range from 1 to 50 Hz. At each temporal frequency the observer adjusted contrast to the threshold of detectability (not smoothness) to give a contrast sensitivity curve for temporal frequency. The results are shown by the smooth curves, without individual data points, in Fig. 7. The data points appearing in Fig. 7 are values calculated from the set of measurements immediately preceding (Fig. 6) in which contrast was adjusted until sampled motion appeared smooth (if ever it did). The data points are the calculated contrasts of the lowest frequency components of motion introduced by sampling (S_f–F_t) which are always those of greatest amplitude and almost always those of greatest visibility. It will be observed that the data points fit closely on the temporal contrast sensitivity functions (smooth curves), suggesting that sampled motion appears smooth when contrast is reduced to the level at which the artefacts introduced by sampling just become invisible. This suggestion is reinforced by the observation that at high levels of contrast multiple components of motion, some very swift and some in the reverse direction, are visible when motion is sampled.

DISCUSSION

The results we report here demonstrate that for drifting gratings of any combination of spatial and temporal frequency, and at any contrast, there is a jump size at which sampled and smooth motion are indistinguishable on the closest scrutiny. The upper bound on this jump size is substantial at low spatial frequencies, up to 6 deg, but small at high spatial frequencies, as little as 20 sec of arc. The bound on jump size is never as great as the Nyquist limit (half the spatial period) at which aliasing (the "wagon wheel effect") begins. It is also influenced by temporal frequency, being in general greater at

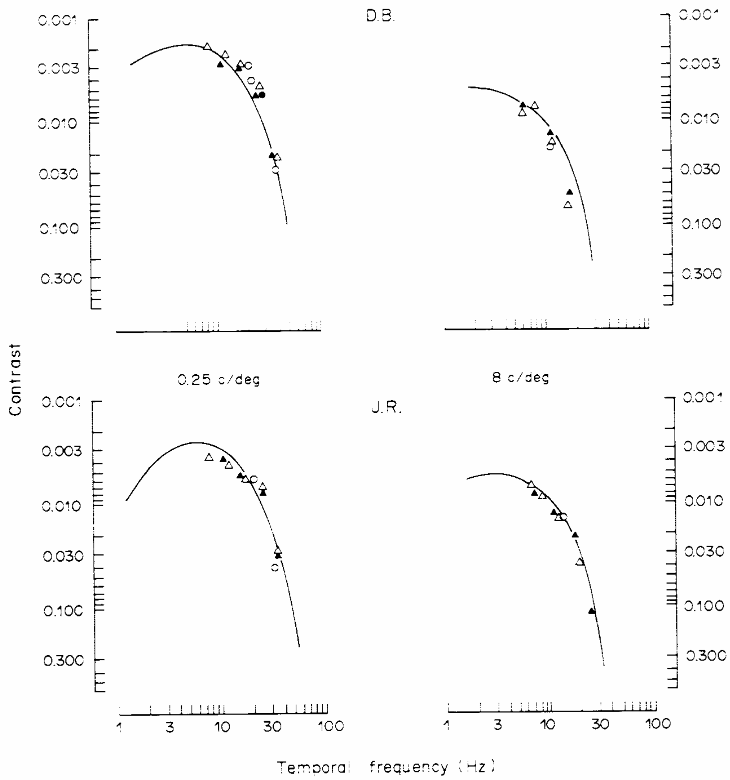

Fig. 7. The symbols refer to the contrast of the most visible spurious harmonic introduced by sampling at the threshold for smooth motion, as a function of the temporal frequency of those harmonics. The results are calculated from Fig. 6 by applying equation (3). The symbols refer to the same drift frequencies as in Fig. 6. The solid curves are derived from measurements of threshold contrast for detection of 0.25 and 8 c deg gratings, as a function of drift frequency.

high than at low temporal frequencies, and by contrast, greater at low than at high contrasts. These facts suggest that the limit on the frequency of sampling of motion, considered spatially or temporally, is set by factors over and above the limit at which aliasing begins.

Sampling preserves motion at the fundamental frequency but it also introduces artefactual components of motion, symmetrically placed about integral multiples of the frequency of sampling. These artefacts are visible at high contrasts as components moving at high velocities along with the fundamental, and sometimes as components moving in the reverse direction. They may make motion at the fundamental drift frequency appear jerky, slow or otherwise distorted. A comparison of the calculated contrast of the artefact of highest contrast (when contrast is reduced to the point at which motion appears smooth) with the temporal contrast sensitivity curve reveals that motion appears smooth just when this artefact becomes invisible. In other words, sampled motion appears smooth if sampling exceeds the Nyquist limit and if sampling artefacts are below their individual thresholds. That smoothness of motion is entirely predictable by the visibility of the artefactual harmonics introduced by sampling is consistent with linearity at threshold of motion detectors, at least at an early stage in the process of motion detection.

The pattern of results for localised Gabor wave packets which traverse the screen in single sweeps is very similar to the pattern for gratings, which cover the whole screen. The upper bound on jump size for Gabor wave packets, as for gratings, is larger when they themselves are larger (lower in fundamental frequency) and smaller when they are smaller. The range of jump sizes, 3 deg down to 30″, is almost as large as for gratings, being only slightly truncated at both ends. Upper bounds are reasonably consistent with the frequency spectrum of the wave packets, which has a Gaussian spread about the fundamental, lending credibility to the proposition that the same mechanisms operate to sense motion both for gratings and wave packets.

The appearance of motion in cinematic or stroboscopic displays has been considered a puzzle since the early part of this century when it was first investigated systematically (Wertheimer, 1912; Korte, 1915). Several explanations have been framed on the supposition that motion is derived from stationary images or frames by cognitive (e.g. Kolers, 1972; Johannson, 1975) or computational (e.g. Anstis, 1970; Braddick, 1974; Ullman, 1979) processes.

Several new models, couched in frequency terms, have been proposed to explain the processes by which vision analyses motion. They highlight the issue of sampling. Adelson and Bergen (1985) have proposed an energy model built from pairs of linear filters, oriented in space–time and tuned in spatial frequency. Van Santen and Sperling (1984, 1985) have proposed an elaborated Reichardt model, the basic units of which are pairs of sub-units tuned to opposite directions. Watson and Ahumada (1985) propose a two-stage model made up of scalar motion sensors at the first stage, and vector motion sensors at the second. All three models (which may be equivalent in some respects) employ components tuned both in spatial and in temporal frequency and so potentially sensitive both to components of motion preserved by sampling and to sampling artefacts.

We have described a space-time model (Burr, 1983; Burr and Ross, 1985; Burr *et al.*, 1986) in which motion is sensed and analysed by mechanisms having receptive fields extended in space and in time. The fields have an orientation and an opponent structure sensitising them to spatial patterns of a particular size moving at a particular velocity. We have also argued that detectors of this kind, tuned to spatial and temporal frequency, should sense intermittently sampled motion, cinematic or stroboscopic, just as well as smooth motion, given sampling of sufficient frequency, or equivalently, jump sizes within the spatial boundaries of the appropriate fields. Our results for drifting gratings imply that sampled motion is detected by exactly the same mechanisms as smooth motion, not by an analysis of stationary images and changes in them from time to time.

Several types of apparent motion (phi, alpha, beta etc.) have been distinguished (Korte, 1915; Neuhaus, 1930), and more recently a distinction has been drawn between two types of process presumed to underlie the appearance of motion, one with a short range, up to 15 min, and the other with a long range (Braddick, 1974). We find a continuum of "ranges", that is of upper bounds on jump size, from some seconds of arc to several degrees, moreover with a very strict criterion, the indistinguishability of sampled motion from smooth. Our results are also consistent with studies which show that the putative short range limit increases with field size (Baker and Braddick, 1982; Chang and Julesz, 1983), with element size (Petersick *et al.*, 1983) and sparsity of elements (Ramachandran and Anstis, 1983). In each case an increasing emphasis on components of lower spatial frequency is accompanied by an increase in permissible jump size.

The spatial frequency preference of motion detectors varies considerably, from 0.025 to 15 c deg (Anderson and Burr, 1985a). The spatial extent of the receptive fields of the detectors (measured by a psychophysical summation technique) also varies considerably, from 2′ arc for those preferring 15 c deg to 7 deg for those preferring 0.025 c deg (Anderson and Burr, 1985b). All intermediate sizes are represented, with no indication of a dichotomy which may parallel the putative short and long range processes. The continuum of ranges of receptive field sizes presumably provides the basis for the continuum of threshold jump sizes that we report here.

The theoretical import of this study is to break down distinctions between real and apparent motion and to establish the conditions under which sampled motion appears smooth. The practical implication is to provide a basis for determining sampling rates and sampling regimes required to broadcast and to store and replay records of action so that it appears smooth and natural to the human observer.

Acknowledgements—MCM was a National Research Fellow and DCB a QEII Research Fellow, both from the Australian Department of Science during the duration of these experiments. We thank both the ARGS and NH & MRC for financial support.

REFERENCES

Adelson E. H. and Bergen J. R. (1985) Spatiotemporal energy models for the perception of motion. *J. opt. Soc. Am. A* **2,** 284–299.

Anderson S. J. and Burr D. C. (1985a) Spatial and temporal selectivity of the human motion detection system. *Vision Res.* **25,** 1147–1154.

Anderson S. J. and Burr D. C. (1985b) Receptive field sizes of human motion detectors. *Perception* **14,** A19.

Anstis S. M. (1970) Phi movement as a subtraction process. *Vision Res.* **10,** 1411–1430.

Baker C. L. and Braddick O. J. (1982) The basis of area and dot number effects in random dot motion perception. *Vision Res.* **22,** 1253–1257.

Braddick O. (1974) A short-range process in apparent motion. *Vision Res.* **14,** 519–527.

Burr D. C. (1979) On the visibility and appearance of objects in motion. Ph.D. thesis, Univ. of Cambridge.

Burr D. C. (1983) Human vision in space and time. *Proc. Int. Union Physiol. Sci.* **15,** S10.04.

Burr D. C. and Ross J. (1985) Visual analysis during motion. In *Vision, Brain and Cooperative Computation* (Edited by Arbib & Hanson) M.I.T. Press. In press.

Burr D. C. and Ross J. (1982) Contrast sensitivity at high velocities. *Vision Res.* **23,** 3567–3569.

Burr D. C., Ross J. and Morrone M. C. (1986) Seeing objects in motion. *Proc. R. Soc., Lond.* In press.

Burt P. and Sperling G. (1981) Time, distance and feature trade-offs in visual apparent motion. *Psychol. Rev.* **88,** 171–195.

Campbell F. W. (1980) Recent attempts to link psychophysics with neurophysiology in vision research. *Trans. Ophthal. Soc. U.K.* **99,** 326–332.

Chang J. J. and Julesz B. (1983) Displacement limits for spatial frequency filtered random-dot cinematograms in apparent motion. *Vision Res.* **23,** 1379–1385.

Fahle M. and Poggio T. (1981) Visual hyperacuity: spatiotemporal interpolation in human vision. *Proc. R. Soc. B* **213,** 451–477.

Johansson G. (1975) Visual motion perception. *Scient. Am.* **232,** 76–88.

Kolers P. A. (1972) *Aspects of Motion Perception.* Pergamon Press, Oxford.

Korte A. (1915) Kinematokipische Untersuchungen. *Z. Psychol.* **72,** 193–206, 271–296.

Marr D. and Ullman S. (1979) Directional selectivity and its use in early visual processing. *Proc. R. Soc., Lond.* **B204,** 301–328.

Nakayama K. and Silverman G. H. (1984) Temporal and spatial characteristics of the upper displacement limit for motion in random dots. *Vision Res.* **24,** 293–299.

Neuhaus W. (1930) Experimentelle Untersuchung der Scheinbewegung. *Archs ges. Psychol.* **75,** 315–458.

Pearson D. E. (1975) *Transmission and Display of Pictorial Information.* Pentech. London.

Petersick J. T., Pufahl R. and Krasnoff E. (1983) Failure to find an absolute retinal limit of a putative short-range process in apparent motion. *Vision Res.* **23,** 1663–1670.

Ramachandran V. S. and Anstis S. M. (1983) Displacement thresholds for coherent apparent motion in random dot-patterns. *Vision Res.* **23,** 1719–1724.

Van Santen J. P. H. and Sperling G. (1984) Temporal covariance model of human motion perception. *J. opt. Soc. Am. A* **1,** 451–473.

Van Santen J. P. H. and Sperling G. (1985) Elaborated Reichardt detectors. *J. opt. Soc. Am. A* **2,** 300–321.

Tyler C. W. (1974) Observations on spatial frequency doubling. *Perception* **3,** 81–86.

Ullman S. (1979) *The Interpretation of Visual Motion.* MIT Press, Cambridge, Mass.

Watson A. B. and Ahumada A. J. (1985) Model of human visual-motion sensing. *J. opt. Soc. Am. A* **2,** 322–340.

Wertheimer M. (1912) Experiementelle studien uber das Sehen von Bewegung. *Z. Psychol.* **61,** 151–265.

Zeeman W. P. C. and Roelofs C. O. (1953) Some aspects of apparent motion. *Acta psychol.* **9,** 159–181.